

1 **Supplementary Information**

2 **A Hybrid Transistor with Transcriptionally Controlled Computation and Plasticity**

3  
4 Yang Gao<sup>1</sup>, Yuchen Zhou<sup>2,3</sup>, Xudong Ji<sup>4,5</sup>, Austin J. Graham<sup>1,6</sup>, Christopher M. Dundas<sup>1,7</sup>, Ismar  
5 E. Miniel Mahfoud<sup>1</sup>, Bailey M. Tibbett<sup>1</sup>, Benjamin Tan<sup>3,8</sup>, Gina Partipilo<sup>1</sup>, Ananth Dodabalapur<sup>2,3</sup>,  
6 Jonathan Rivnay<sup>4,5</sup>, Benjamin K. Keitz<sup>1\*</sup>

7  
8 <sup>1</sup>McKetta Department of Chemical Engineering, University of Texas at Austin, Austin, TX,  
9 78712, USA

10 <sup>2</sup>Department of Electrical and Computer Engineering, The University of Texas at Austin, Austin,  
11 TX, 78712, USA

12 <sup>3</sup>Microelectronics Research Center, The University of Texas at Austin, Austin, TX, 78758, USA

13 <sup>4</sup>Department of Biomedical Engineering, Northwestern University, Evanston, IL, 60208, USA

14 <sup>5</sup>Simpson Querrey Institute, Northwestern University, Chicago, IL, 60611, USA

15 <sup>6</sup>Department of Pharmaceutical Chemistry, University of California San Francisco, San  
16 Francisco, CA, 94158, USA

17 <sup>7</sup>Department of Biology, Stanford University, Stanford, CA 94305, USA

18 <sup>8</sup>Department of Chemistry, University of Texas at Austin, Austin, TX, 78712, USA

19  
20 \*To whom correspondence should be addressed: keitz@utexas.edu  
21  
22  
23  
24  
25  
26  
27  
28  
29  
30  
31  
32  
33  
34  
35  
36  
37  
38  
39  
40  
41  
42  
43  
44

45	<b>Table of Contents</b>	
46	<b>Methods</b> .....	<b>3</b>
47	<b>Chemicals and Reagents</b> .....	3
48	<b>Bacteria Strains and Culture</b> .....	3
49	<b>Device Fabrication</b> .....	3
50	<b>Device Operation and Electrochemistry</b> .....	4
51	<b>Inoculation Procedure</b> .....	5
52	<b>Spectroscopy</b> .....	6
53	<b>Fluorescence Microscopy</b> .....	6
54	<b>Atomic Force Microscopy</b> .....	7
55	<b>OECT Data Processing</b> .....	7
56	<b>Statistical Methods</b> .....	8
57	<b>Tables</b> .....	<b>9</b>
58	<b>Table S1. Strains and plasmids used in this study</b> .....	9
59	<b>Table S2. Shewanella Basal Medium (SBM) formulation</b> .....	10
60	<b>Table S3. Relevant statistical values</b> .....	10
61	<b>Supplementary Figures</b> .....	<b>11</b>
62	<b>Figure S1. Cell viability and growth in OECTs under varying culture and operation conditions</b> .....	11
63	<b>Figure S2. OECT channel current <math>I_{DS}</math> reduction in abiotic and different cell metabolic states</b> .....	12
64	<b>Figure S3. OECT de-doping investigated using electrochemical and spectroscopy methods</b> .....	13
65	<b>Figure S4. OECT responses to <math>\Delta mtrC</math> strains carrying NAND and NOR Boolean gate plasmids</b> .....	14
66	<b>Figure S5. Modulation of the OECT synaptic behavior with varying pulse conditions and strains</b> .....	15
67	<b>Figure S6. Cartoon illustration of the major OECT channel fabrication and assembly steps</b> .....	16
68	<b>Figure S7. Morphological characterization of PEDOT:PSS channel and gate-tip coating</b> .....	17
69	<b>Figure S8. OECT response to different extracellular electron transfer (EET) mechanisms</b> .....	18
70	<b>Figure S9. Channel current <math>I_{DS}/I_{DS0}</math> curves of strains carrying the Boolean logic gates plasmids</b> .....	19
71	<b>Figure S10. Growth curves of mutant strains carrying the Boolean logic gates plasmids</b> .....	19
72	<b>Figure S11. Measured channel currents <math>I_{DS}</math> and electrode potentials responding to gate pulses</b> .....	20
73	<b>Figure S12. Paired-pulse responses of abiotic OECTs at varying electrochemical doping states</b> .....	20
74	<b>Figure S13. Electrochemical response of the hybrid OECTs under varying oxygen conditions</b> .....	21
75	<b>References</b> .....	<b>21</b>

76

## 77 **Methods**

78

### 79 **Chemicals and Reagents**

80

81 PEDOT:PSS aqueous suspension (Clevios™ PH1000, Heraeus Epurio LLC), ethylene glycol  
82 (anhydrous 99.8%, Sigma-Aldrich), sulfuric acid (H<sub>2</sub>SO<sub>4</sub>, 95.0-98.0 %, Sigma-Aldrich), hydrogen  
83 peroxide (H<sub>2</sub>O<sub>2</sub>, 30 wt% in water, Sigma-Aldrich), sodium DL-lactate (NaC<sub>3</sub>H<sub>5</sub>O<sub>3</sub>, 60% in water,  
84 TCI), sodium fumarate (Na<sub>2</sub>C<sub>4</sub>H<sub>2</sub>O<sub>4</sub>, 98%, VWR), HEPES buffer solution (C<sub>8</sub>H<sub>18</sub>N<sub>2</sub>O<sub>4</sub>S, 1 M in  
85 water, pH = 7.3, VWR), potassium phosphate dibasic (K<sub>2</sub>HPO<sub>4</sub>, Sigma-Aldrich), potassium  
86 phosphate monobasic (KH<sub>2</sub>PO<sub>4</sub>, Sigma-Aldrich), sodium chloride (NaCl, VWR), ammonium  
87 sulfate ((NH<sub>4</sub>)<sub>2</sub>SO<sub>4</sub>, Fisher Scientific), magnesium(II) sulfate heptahydrate (MgSO<sub>4</sub>·7H<sub>2</sub>O, VWR),  
88 Wolfe's Trace Mineral Mix (ATCC), casamino acids (VWR), isopropyl β-D-1-  
89 thiogalactopyranoside (IPTG, Teknova), anhydrotetracycline hydrochloride (aTc, Sigma-Aldrich),  
90 3-oxohexanoyl-homoserine lactone (OC6, Sigma-Aldrich), kanamycin sulfate (C<sub>18</sub>H<sub>38</sub>N<sub>4</sub>O<sub>15</sub>S,  
91 Growcells), Riboflavin 5' -monophosphate sodium salt hydrate (>93 %, TCI), and LIVE/DEAD®  
92 BacLight™ Stain (L7012, Invitrogen), were used as received. Two-part silicone elastomer  
93 (Sylgard™ 184, Electron Microscopy Sciences) was used according to manufacturer instructions.  
94 All media components were autoclaved or sterilized using 0.22 μm PES filters.

95

### 96 **Bacteria Strains and Culture**

97

98 Bacterial strains and plasmids are listed in Table S1. Cell cultures were prepared from bacterial  
99 stocks stored in 20% glycerol at -80 °C. The stocks were streaked onto agar plates containing  
100 LB (for wild-type and knockout strains) or LB with 25 μg/mL kanamycin (for plasmid-harboring  
101 strains), and subsequently grown overnight at 30 °C for *Shewanella* and 37 °C for *E. coli*. Single  
102 colonies from the plates were picked and inoculated into *Shewanella* Basal Medium (SBM, Table  
103 S2) amended with 0.05% trace mineral supplement, 0.05% casamino acids, and supplemented  
104 20 mM sodium lactate (2.85 μL of 60% w/w sodium lactate per 1 mL culture) for *Shewanella* and  
105 20 mM glucose (10 μL of 2 M glucose per 1 mL culture) for *E. coli* as the electron donor, unless  
106 otherwise noted. Aerobic cultures were pregrown in 15 mL culture tubes at 30 °C and 250 rpm  
107 shaking. Anaerobic cultures were pregrown using the same procedure outlined above, but with  
108 argon purged growth medium in a nitrogen-filled glovebox (S1200, Vigor) and supplemented with  
109 40 mM sodium fumarate (40 μL of 1 M sodium fumarate per 1 mL culture) as the electron acceptor.  
110 Additional 25 μg/mL kanamycin (10 μL of 2.5 mg/mL kanamycin per 1 mL culture) was  
111 supplemented to the pregrowth medium of plasmid-harboring strains. Aerobically pregrown  
112 cultures were washed 3x using the sterile SBM growth medium and adjusted to an OD<sub>600</sub> of 1-3.5  
113 (NanoDrop 2000C) before being transferred into the glovebox. For steady-state protein  
114 expression, strains were pregrown anaerobically without inducer(s) for 6 h before being diluted  
115 1:25 into inducer-containing media (from 1000x stocks) and grown for 18-24 hours.

116

### 117 **Device Fabrication**

118

119 Three versions of the OECTs were used: small channel OECTs, 2-electrode versions of the small  
120 channel OECT without the gate, and a large channel OECT. The small channel OECTs were  
121 used for the majority of experiments with the following exceptions. In direct channel reduction  
122 experiments (Figure 2h, Figure S3g), the 2-electrode versions of the small channel OECT were  
123 used and noted as 2-electrode devices or no gate. In UV-vis spectroscopy (Figure 2g, Figure S3c  
124 – S3e), the large channel OECTs were used to fit the laser aperture of the instrument. The large  
125 channel OECTs were labeled as 'large channel OECTs' and the small channel OECTs were noted  
126 as original three-terminal OECTs or without any specific naming. OECTs were fabricated  
127 according to prior work<sup>1</sup>. Quartz microscopic slides (FQ-S-003, AdValue Technology) were  
128 cleaned with soapy water, acetone, and isopropyl alcohol, and dried with nitrogen before oxygen  
129 reactive-ion etching (RIE, 150 W, 50 sccm, 120 s). Quartz slides were coated with a photoresist  
130 layer (AZ5209E) and lithographically patterned to define the electrode layout. Subsequently, Au  
131 electrodes (100 nm) with a Ti adhesion layer (10 nm) were thermally evaporated on the quartz  
132 slides, and excess materials were removed with acetone lift-off. Another photolithographic pattern  
133 was formed to define the PEDOT:PSS region over the channel and the tip of the gate to obtain a  
134 width/length of 150  $\mu\text{m}$  x 10  $\mu\text{m}$  and 500  $\mu\text{m}$  x 500  $\mu\text{m}$ , respectively. The PEDOT:PSS (Clevios<sup>TM</sup>  
135 PH1000) was filtered (0.22  $\mu\text{m}$  PES filters) and spun cast on the patterned quartz slides, followed  
136 by hot plate drying at 90 °C for 15 min and acetone lift-off. To increase the conductivity,  
137 PEDOT:PSS films were immersed in ethylene glycol at 90 °C for 3 min over a hot plate. The as-  
138 fabricated PEDOT:PSS film had an average thickness of 26.5 nm for the channel and 38.3 nm  
139 for the gate-tip layer. Polydimethylsiloxane (PDMS, Sylgard<sup>TM</sup> 184) with 9 % wt curing agent was  
140 drop cast and cured for 48 hours at room temperature to ensure surface smoothness. The OECT  
141 chambers and fluid access ports in the PDMS sheets were manually cut with a hole punch.

142  
143 The OECTs with the larger channel size were only used for UV-vis measurement. The electrodes  
144 were fabricated in the same way as the smaller OECT. The PEDOT:PSS channel was fabricated  
145 by drop-casting 80  $\mu\text{L}$  PEDOT:PSS over the entire slide, followed by 20 minutes of air-drying and  
146 heating at 90°C for 20 minutes. Afterward, the excessive PEDOT:PSS film was removed with  
147 cotton swabs soaked with 70% ethanol. Conductivity enhancement was achieved by EG  
148 treatment of 10 min at 90 °C. Silicon spacers (0.5 mm, GBL664581, Sigma-Aldrich) were hand  
149 cut to create the OECT chambers and only used with the large channel OECTs.

## 150 151 ***Device Operation and Electrochemistry***

152  
153 Shewanella Basal Medium (SBM) amended with 0.05% casamino acids and 1X Wolfe's Trace  
154 Mineral Mix was used as the base electrolyte except for the carbon source comparison  
155 experiments (Figure 2e, Figure S2d) where the SBM was only amended with 1X Wolfe's Trace  
156 Mineral Mix. When noted, the SBM was further supplemented with 40 mM sodium fumarate to  
157 support cell growth. Before each experiment, the OECT slides and PDMS sheets were autoclaved  
158 separately and assembled in the biosafety cabinet. OECT experiments were conducted in a  
159 nitrogen-filled glovebox to create the anaerobic condition except for UV-vis spectroscopy which  
160 was conducted under ambient conditions. Media and solutions stocks were purged with argon for  
161 15 min and stored in the glovebox. A multichannel potentiostat (MultiPalmSens4, PalmSens BV)  
162 was used for the electrochemical measurements. During continuous OECT operation, unless

163 otherwise noted, the gate ( $V_{GS}$ ) and drain ( $V_{DS}$ ) voltages were biased at 0.2V and -0.05 V,  
164 respectively. Transfer curves were measured with a gate scan rate of 20 mV/s, except in the  
165 artificial synaptic hysteresis measurement where a rate of 10 mV/s was used. For all the  
166 experiments, OECTs were stabilized in the glovebox with abiotic electrolytes and constant bias  
167 voltages for 72 hours before inoculation or measurements.

168  
169 In the electrode potential measurements with Ag/AgCl pellet reference electrode (550010, A-M  
170 Systems), the Ag/AgCl electrodes were directly inserted into the OECT chamber without salt  
171 bridges. The same Ag/AgCl pellet electrodes were used as the gate for the large channel OECTs  
172 in abiotic UV-vis measurements. Hybrid OECT experiments with electroactive bacteria were  
173 conducted between 18 - 36 hours after inoculation (initial  $OD_{600}$  at 0.01). Synaptic measurements  
174 were conducted after  $I_{DS}$  was stabilized for at least 1 minute at  $V_{GS} = 0$  V.

175

### 176 ***Inoculation Procedure***

177  
178 For aerobic culture growth, SBM supplemented with 20 mM lactate was used for cell growth.  
179 Following aerobic overnight growth, the cultures were triple-washed by centrifugation using the  
180 same growth medium to remove byproducts. The optical density of the washed cultures was  
181 measured before transferring them into the glovebox. side the glovebox, the cell cultures were  
182 diluted to create an intermediate inoculum with a cell density 10-fold higher than the target OD for  
183 final inoculation. This dilution used the same electrolyte solution that filled the OECT. Finally, the  
184 OECTs were inoculated using a 1:9 volume ratio of the intermediate cell culture to the OECT  
185 electrolyte. For instance, *S. oneidensis* supplemented with 1  $\mu$ M exogenous FMN with inoculum  
186  $OD_{600}$  of 0.05 was prepared from aerobically grown cell cultures. The triple-washed cell cultures  
187 (average  $OD_{600}$  at 3.38) were brought into the glovebox and diluted to the intended  $OD_{600}$  of 0.5  
188 with SBM supplemented with 1  $\mu$ M exogenous FMN, creating the intermediate cultures. Then 5  
189  $\mu$ L of these intermediate cultures were inoculated into the OECTs containing 45  $\mu$ L of SBM  
190 supplemented with 1  $\mu$ M FMN, achieving a final inoculation  $OD_{600}$  at 0.05.

191  
192 For steady-state expression conditions, cells were anaerobically cultured in SBM supplemented  
193 with 20 mM lactate and 40 mM fumarate, along with specific inducer(s). To maintain consistent  
194 induction strength and to prevent cell growth from affecting OECT readouts, electrolyte in the  
195 OECTs were SBM supplemented with 20 mM lactate and specific inducer(s), but lacked fumarate.  
196 Prior to induction, strains were grown statically and anaerobically without inducer(s) for 6 hours.  
197 Subsequently, cell cultures were diluted 1:25 into media containing inducers (prepared from  
198 1000x concentrated stocks) and incubated for an additional 18-24 hours. After this induction  
199 period, the cell cultures were directly inoculated into the OECTs at a 100-fold overall dilution  
200 without prior washing. Specifically, cells were first diluted 10-fold with the fumarate-free OECT  
201 electrolyte forming the intermediate cultures. The final inoculation of the OECTs was achieved by  
202 adding the intermediate cell culture to the OECT electrolyte at a 1:9 volume ratio.

203  
204 In the carbon source experiment, SBM amended with 1X Wolfe's Trace Mineral Mix was used as  
205 the base electrolyte. Aerobically grown *S. oneidensis* MR-1 cells culture were triple-washed with  
206 SBM without a carbon source, then the cell cultures were kept at room temperature for 3 hours to

207 induce starvation conditions<sup>2</sup>. Afterward, cell cultures were washed again and their OD<sub>600</sub> was  
208 measured. Subsequently, cell cultures were brought into the glovebox and diluted to obtain the  
209 intermediate stocks with an intended OD<sub>600</sub> of 0.1. The dilutions were performed with SBM  
210 supplemented with either 20 mM lactate, 20 mM pyruvate, 20 mM acetate, or no carbon source.  
211 Finally, the intermediate stocks were inoculated into OECTs containing the SBM supplemented  
212 with the respective carbon source or no carbon source at a ratio of 1:9, achieving a final  
213 inoculation OD<sub>600</sub> of 0.01.

214

215 In cell viability experiments, aerobically grown *S. oneidensis* MR-1 cell cultures were triple-  
216 washed with SBM supplemented with 20 mM lactate. For *E. coli* cultures, the lactate was replaced  
217 with 20 mM glucose. The densities for the washed cell cultures were measured by OD<sub>600</sub> and the  
218 *S. oneidensis* cultures were allocated to 3 parts: live, heat-killed, and lysed cells. Heat-killed cells  
219 were obtained by incubating at 80 °C for 20 min. Lysed cells were obtained by sonication (Qsonica  
220 55, Qsonica LLC) for 90 s at 4 °C. The output power was set to 15 W with “ON” and “OFF” intervals  
221 of 10 s and 5 s, respectively. Then cell cultures were brought into the glovebox and diluted with  
222 SBM supplemented with 20 mM lactate to obtain the intermediate cultures at an intended OD<sub>600</sub>  
223 of 0.1. The intermediate cultures were inoculated into the OECTs at a ratio of 1:9, achieving a  
224 final inoculation OD<sub>600</sub> of 0.01. The *S. oneidensis* supernatants were obtained by filtering (0.22  
225 µm PES filters) the cell cultures (initial OD<sub>600</sub> at 0.01) anaerobically grown in the glovebox with  
226 SBM supplemented with 20 mM lactate. The entire volume of OECT electrolyte was replaced with  
227 the supernatant during inoculation.

228

### 229 **Spectroscopy**

230

231 The UV-Vis spectroscopy of the PEDOT:PSS channel was measured from 190 nm to 1100 nm  
232 (Agilent 8453 UV-Visible Spectroscopy System). A custom sample holder was 3D printed to fit  
233 the OECT slides to the instrument. Measurements were blanked with devices lacking the  
234 PEDOT:PSS channel. When bacteria cells were present in the sample, the blank devices were  
235 likewise inoculated with the same inoculum.

236

### 237 **Fluorescence Microscopy**

238

239 Microscopy was performed using a Nikon Ti2 Eclipse inverted epifluorescence microscope.  
240 Immediately after the 24-hour operation in the glovebox, OECTs were gently washed 2x by  
241 refreshing the electrolyte with the sterile SBM supplemented with 0.05% trace mineral supplement,  
242 0.05% casamino acids. Then, the PDMS sheets were replaced with a 0.5 mm silicon spacer to  
243 ensure the sample thickness was compatible with the working distance of the microscope.  
244 Subsequently, the OECTs were gently washed with SBM containing 0.05% trace mineral  
245 supplement, 0.05% casamino acids, and LIVE/DEAD<sup>®</sup> BacLight<sup>™</sup> Stain mix (3 µL of SYTO 9 and  
246 propidium stocks per 1 mL) at a final solution volume of 10 µL per OECT chamber. The OECTs  
247 were then sealed with coverslips, covered with aluminum foil, and transferred out of the glovebox  
248 for microscope imaging. Bacterial counts were performed using ImageJ software.

249

## 250 **Atomic Force Microscopy**

251  
252 The AFM scans were conducted using a DriveAFM (Nanosurf AG). The cantilevers (Dyn190Al)  
253 were driven with the photothermal laser (CleanDrive) under dynamic mode. OECTs were  
254 randomly selected from two fabrication batches: 3 slides of the as-fabricated OECTs (8 OECTs  
255 per slide) were used as pre-inoculation samples, and 3 cleaned OECT slides post the 48-hour  
256 inoculation served as post-inoculation samples. Two OECTs per slide were randomly chosen for  
257 AFM scans using Nanosurf CX software for data acquisition. Images for PEDOT:PSS film  
258 thickness were acquired at 90  $\mu\text{m}$  x 90  $\mu\text{m}$  and processed with Nanosurf CX software to correct  
259 background variations. Topology and phase images were acquired at 500 nm x 500 nm and  
260 analyzed without further process. Grain sizes were fitted by the Watershed method with the  
261 resulting histograms generated using Gwyddion software.

## 263 **OECT Data Processing**

264  
265 Measured OECT data were processed using GraphPad Prism9 and MATLAB (R2021b update  
266 1). The measured  $I_{DS}$  data were normalized to the initial value before inoculation ( $I_{DS0}$ ) before  
267 fitting. The  $I_{DS}$  decay rate constants for all samples except the lysed *S. oneidensis* were obtained  
268 by fitting  $I_{DS}/I_{DS0}$  data with an exponential decay model:

$$269 \quad i_{DS}(t) = e^{k*t} \quad (1)$$

270  
271  
272 Where  $t$  is time in hours,  $k$  is the fitted  $I_{DS}$  decay rate constant. Fitting was performed with the  
273 built-in one phase decay function in GraphPad Prism9. The  $I_{DS}/I_{DS0}$  data for lysed *S. oneidensis*  
274 samples were fitted to a simple linear regression model:

$$275 \quad i_{DS}(t) = I_{DS0} + \beta t \quad (2)$$

276  
277  
278 Where  $t$  is time in hours, the slope  $\beta$  is used as the rate of change. Fitting was performed with  
279 the built-in simple linear regression function in GraphPad Prism9.

280 The response function of FMN concentrations was modeled with a four-parameter logistic  
281 regression function in terms of  $I_{DS}$  decay rate constants (noted here as  $r$ ):

$$282 \quad \frac{r}{R_{max}} = \frac{[S]^n}{\left(K_{\frac{1}{2}}\right)^n + [S]^n} \quad (3)$$

283  
284  
285 Where  $n$  is the Hill coefficient,  $[S]$  is the FMN concentrations,  $R_{max}$  is the maximum rate constant,  
286  $K_{\frac{1}{2}}$  is the half-maximum concentration constant. Fitting was performed with the built-in four-  
287 parameter dose-response function in GraphPad Prism9.

288 In synaptic experiments, MATLAB scripts were used to process the measured data. The  
289 'Vgs\_pulse\_pair.m' script was used to identify and extract the channel current  $I_{DS}$  peak values  
290 using `islocalmax` function (Figure 5d, 5e, 5g - 5i, Extended Data Figure 5a - 5e). The  
291 'IDS\_VGS\_Pul\_long.m' script implemented median filtering to remove pulses and extract the  
292 baseline for channel current  $I_{DS}$  responding to continuous gate pulse inputs. The filtering was

293 achieved by using the medfilt1 function (Figure 5f and Figure S5f). Extracted  $I_{DS}$  curves were  
294 fitted to an exponential model  $b(1)*\exp(b(2)*x(:,1))+b(3)$  with fitnlm function to obtain the rate  
295 constants, where  $b(1)$ ,  $b(2)$ , and  $b(3)$  are fitting coefficients,  $x$  is time in seconds.

296

297 All scripts are available through the Texas Data Repository.

298

### 299 **Statistical Methods**

300

301 Independent samples t-tests were conducted using the built-in t-test function with the unpaired  
302 option in GraphPad Prism9.

303

304 In the 2-input Boolean gate figures (Figure 4c and 4d, Figure 5h and 5i), statistical tests were  
305 performed using R (version 4.2.3) with multcomp package (version 1.4-23). In brief, we employed  
306 a linear model fitting approach to determine the interaction term between the two inputs noted as  
307 Factor1 and Factor2, specifically  $\text{lm}(\text{Results} \sim \text{Factor1} * \text{Factor2} - 1)$ . Then, based on the  
308 significance of the interaction terms, different linear contrasts were tested for general linear  
309 hypotheses, specifically  $\text{glht}(\text{model}, \text{linfc} = \text{contrast})$ . The significance of the interaction term was  
310 examined for  $p < 0.05$ . If the interaction term was significant, the following linear contrasts were  
311 evaluated for each specific logic gate and model parameterization:

312

$$313 \text{ NAND gate: } H_0: \mu_{++} + \frac{-1}{3}(\mu_{--} + \mu_{+-} + \mu_{-+}) = 0 \quad (4)$$

$$314 \text{ NOR gate: } H_0: \frac{-1}{3}(\mu_{++} + \mu_{+-} + \mu_{-+}) + \mu_{--} = 0 \quad (5)$$

315

316 The contrast matrices for the NAND and NOR logic gates in the general linear hypothesis test are  
317 as follows:  $(\frac{2}{3}, -\frac{2}{3}, -\frac{2}{3}, -\frac{1}{3})$  for NAND gate, and  $(-\frac{2}{3}, \frac{2}{3}, \frac{2}{3}, 1)$  for NOR gate.

318 These contrast matrices were calculated by algebraic substitution given the following  
319 coefficient/parameter relationships defined by our parameterization of the linear model,  
320 specifically:  $\mu_{++} = \text{coef}[1]$ ,  $\mu_{+-} = \text{coef}[1] + \text{coef}[3]$ ,  $\mu_{-+} = \text{coef}[2]$ ,  $\mu_{--} = \text{coef}[2] + \text{coef}[3] + \text{coef}[4]$ .  
321 The resulting p-values and the interaction term are outlined in Table S3.

322

323 If the interaction term was not significant, a linear model without interaction was fit to the data,  
324 and the model was tested with new contrast matrix as:  $(1, -\frac{1}{3}, -\frac{1}{3}, -\frac{1}{3})$  for the NAND gate,  
325 and  $(-\frac{1}{3}, 1, -\frac{1}{3}, -\frac{1}{3})$  for the NOR gate. The p-values are outlined in Table S3 without an  
326 interaction term.

327

328

329

330

331

332

333

334

335

336



337 **Tables**

338

339 **Table S1.** Strains and plasmids used in this study.

Strain and Plasmid	Description	Source
<b>Strains</b>		
<i>Escherichia coli</i>		
MG1655	Wild-type strain	Lydia Contreras, University of Texas at Austin
<i>Shewanella oneidensis</i>		
MR-1	MR-1 (ATCC700550) wild type strain	American-Type Culture Collection
$\Delta mtrC$	JG596, deletion of genes <i>mtrC</i> , <i>omcA</i> , and <i>mtrF</i> .	Jeffrey Gralnick, University of Minnesota <sup>3</sup>
$\Delta Mtr$	JG1194, deletion of genes <i>mtrC</i> , <i>omcA</i> , <i>mtrF</i> , <i>mtrA</i> , <i>mtrD</i> , <i>dmsE</i> , <i>SO4360</i> , <i>cctA</i> , and <i>recA</i> .	Jeffrey Gralnick, University of Minnesota <sup>4</sup>
$\Delta bfe$	deletion of genes <i>SO0702</i> .	Jeffrey Gralnick, University of Minnesota <sup>5</sup>
$\Delta lysis$	S2933, deletion of genes <i>SO2966</i> and <i>SO2974</i> .	Lydia Contreras, University of Texas at Austin <sup>6</sup>
<b>Plasmids</b>		
pCD8	Empty Buffer gate	Ref. <sup>7</sup>
pCD24r1	<i>mtrC</i> Buffer gate (sRBS1 <sub>mtrC</sub> )	Ref. <sup>7</sup>
pAT4	<i>Mtr</i> Buffer gate	This work
pNAND- <i>mtrC</i>	<i>mtrC</i> NAND Boolean logic gate	Ref. <sup>8</sup>
pNAND- <i>sfgfp</i>	<i>sfgfp</i> NAND Boolean logic gate	Ref. <sup>8</sup>
pNOR- <i>mtrC</i>	<i>mtrC</i> NOR Boolean logic gate	Ref. <sup>8</sup>
pNOR- <i>sfgfp</i>	<i>sfgfp</i> NOR Boolean logic gate	Ref. <sup>8</sup>

340

341

342 **Table S2.** Shewanella Basal Medium (SBM) formulation

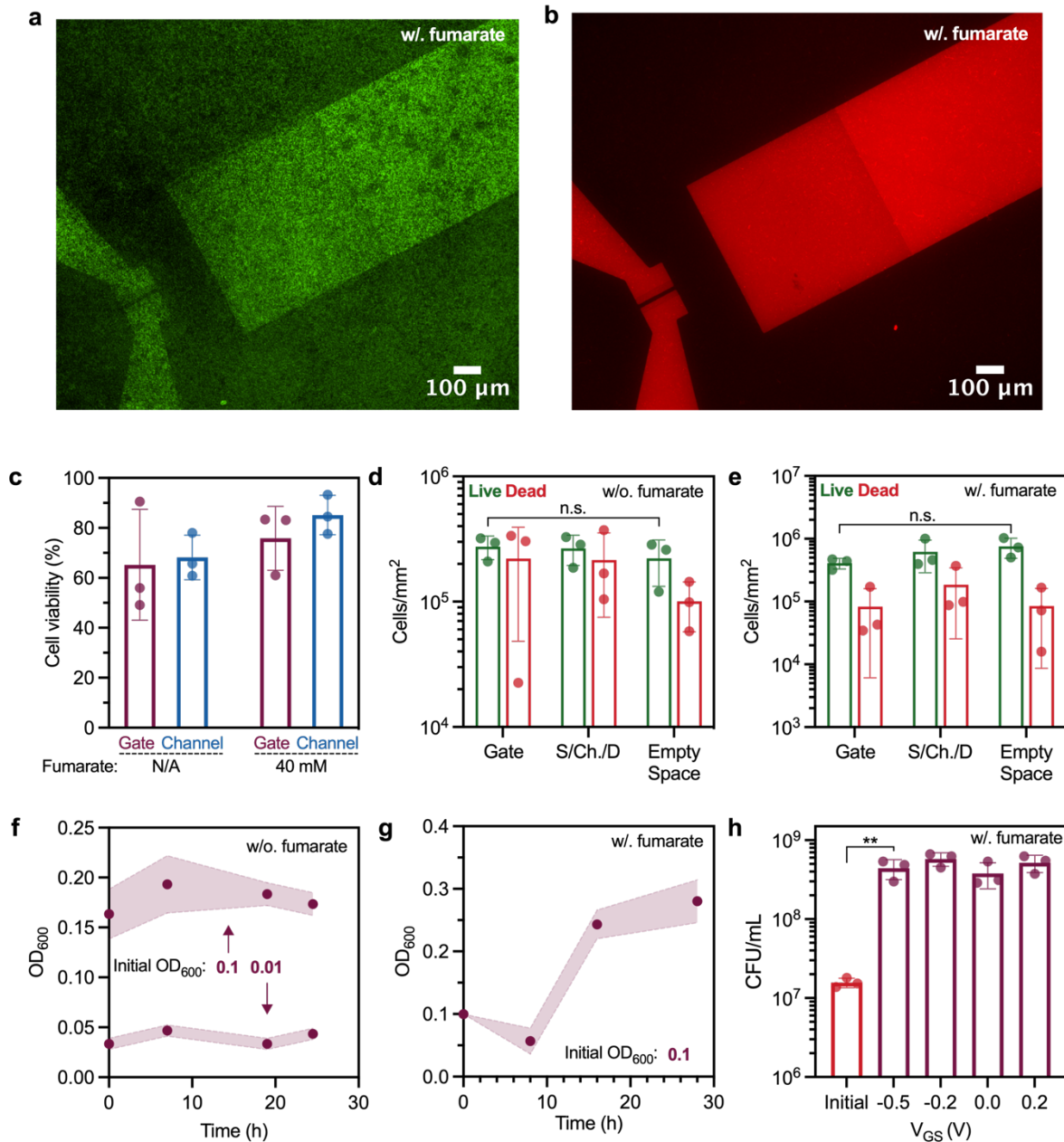
<b>Ingredient</b>	<b>Quantity per 1 L</b>
K <sub>2</sub> HPO <sub>4</sub>	225 mg
KH <sub>2</sub> PO <sub>4</sub>	225 mg
NaCl	460 mg
(NH <sub>4</sub> ) <sub>2</sub> SO <sub>4</sub>	225 mg
MgSO <sub>4</sub> *7H <sub>2</sub> O	117 mg
HEPES	100 mL of 1 M HEPES
Casamino acids	5 mL of 10% casamino acids in ddH <sub>2</sub> O, if needed
Wolfe's Mineral Mix	5 mL of Wolfe's Mineral Mix, if needed
ddH <sub>2</sub> O	Adjust volume to 1 L and pH to 7.2

343

344 **Table S3.** Relevant statistical values

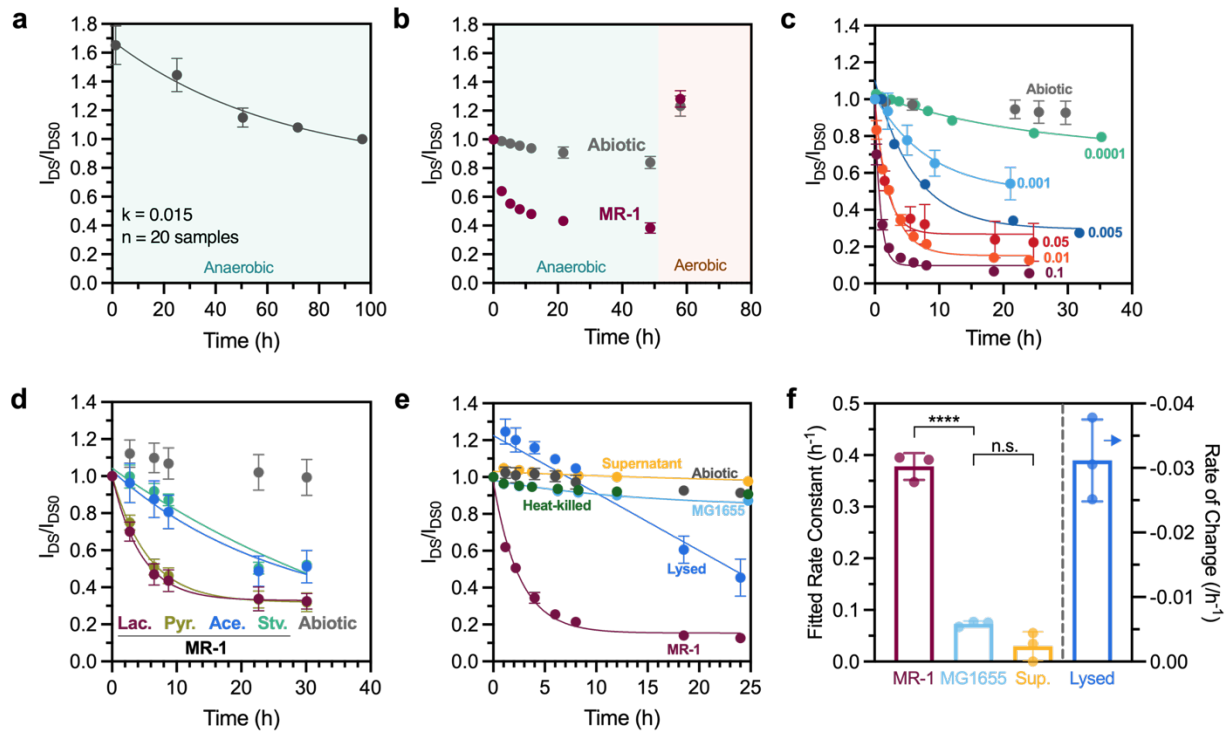
<b>Data Sets</b>	<b>pNAND</b>	<b>pNOR</b>
<b>Source Potential (V<sub>s</sub>)</b>	2-way ANOVA interaction p= 0.00313  Contrast test p = 0.00204	2-way ANOVA interaction p= 1.84 x 10 <sup>-5</sup>  Contrast test p = 2.36 x 10 <sup>-7</sup>
<b>Synaptic Conductance Change (ΔG)</b>	1-way ANOVA contrast test p = 0.00306	1-way ANOVA contrast test p = 0.00152

345  
346  
347  
348  
349  
350  
351  
352  
353  
354  
355  
356  
357  
358  
359



362  
 363 **Figure S1.** Cell viability and growth in OECTs under varying culture and operation conditions.  
 364 Representative fluorescent microscopy images showing OECTs operated with constant drain  
 365 voltage  $V_{DS} = -0.05\text{V}$  and gate voltage  $V_{GS} = 0.2\text{V}$ . Cells were supplemented with 20 mM lactate  
 366 and 40 mM fumarate. LIVE/DEAD<sup>®</sup> BacLight<sup>™</sup> cell assay showing (a) live cells in green and (b)  
 367 dead cells in red. (c) Cell viability derived from the fluorescent microscopy images. (d, e) Cell  
 368 counts over OECT gates, source/channel/drain region (denoted as S/Ch./D), and spaces  
 369 elsewhere (denoted as empty spaces) for cells supplemented with 20 mM lactate, and (d)  
 370 without or (e) with 40 mM fumarate. (f, g) Optical Density at 600 nm ( $OD_{600}$ ) was measured from

371 OECTs biased at  $V_{DS} = -0.05V$  and  $V_{GS} = 0.2V$ , cells supplemented with 20 mM lactate, and (f)  
 372 without or (g) with 40 mM fumarate. The shaded region indicates the range of standard  
 373 deviation. (h) Colony forming units (CFUs) were counted 24 hours after OECTs operation with  
 374 constant  $V_{DS} = -0.05 V$  and  $V_{GS}$  biased at  $-0.5 V$ ,  $-0.2 V$ ,  $0.0 V$ , or  $0.2 V$ . CFU/mL  $p$  value for the  
 375 indicated pair  $p = 0.0042$ . Cells were supplemented with 20 mM lactate and 40 mM fumarate.  
 376 Data show the mean  $\pm$  SD of 3 biological replicates, unpaired two-tailed Student's t-tests were  
 377 performed without adjustments for multiple comparisons, n.s. represents  $p > 0.05$ .  
 378

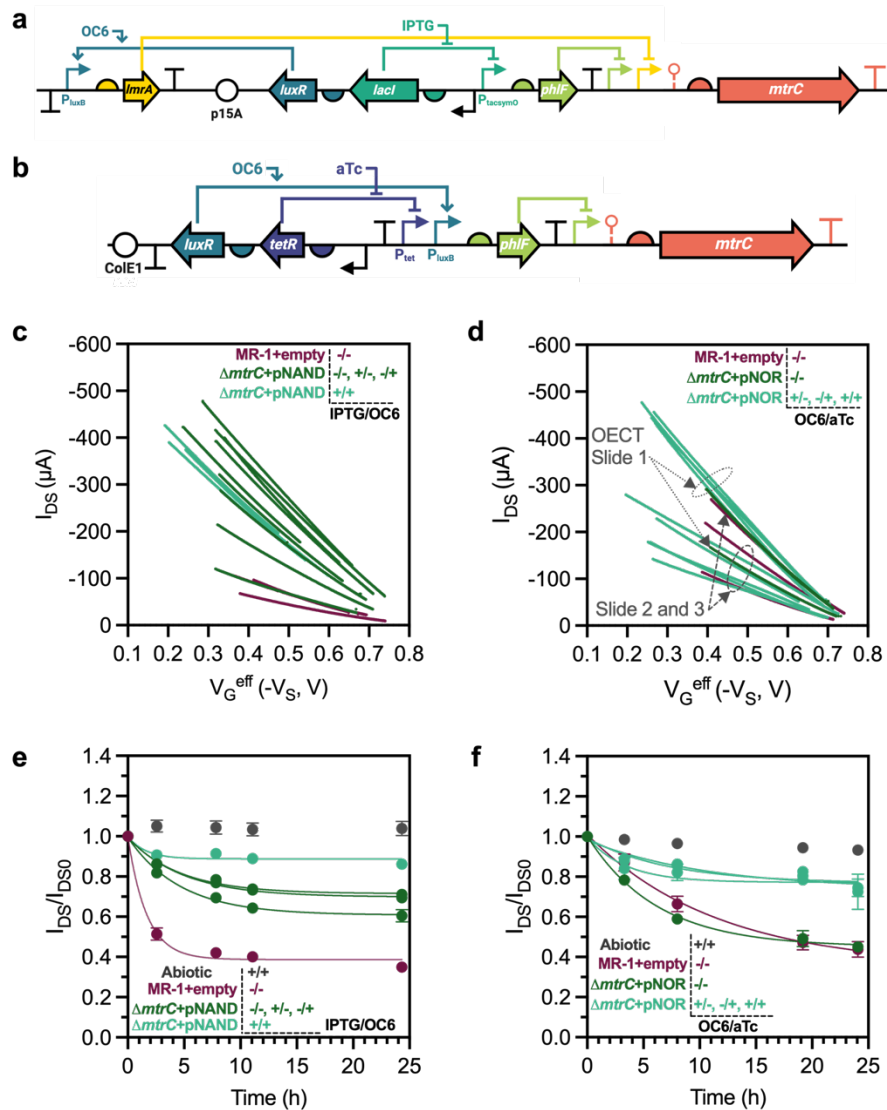


379  
 380 **Figure S2.** OECT channel current  $I_{DS}$  reduction in abiotic and different cell metabolic states.  
 381 The  $I_{DS}/I_{DS0}$  curves during (a) anaerobic stabilization without bacteria cells and (b) 48-hour  
 382 operation followed by exposure to the oxygen in the ambient environment. The  $I_{DS}/I_{DS0}$  curves of  
 383 *S. oneidensis* MR-1 inoculated OECTs with (c) varying inoculation  $OD_{600}$  numbers or (d)  
 384 supplemented with either 20 mM sodium lactate (Lac.), 20 mM sodium pyruvate (Pyr.), or 20 mM  
 385 sodium acetate (Ace.) as the electron donors. No carbon source was supplied to the starved cells  
 386 (Stv.) (e) The  $I_{DS}/I_{DS0}$  curves for living, lysed, and heat-killed *S. oneidensis* MR-1 cells, as well as  
 387 living *E. coli* MG1655 cells. (f) The  $I_{DS}$  decay rate constants for living *S. oneidensis* and *E. coli*  
 388 cells, as well as *S. oneidensis* supernatant. Fitted rate constant  $p$  values for the indicated pair  $p$   
 389  $= 3.8 \times 10^{-5}$ . The lysed *S. oneidensis* curves were fitted using a linear regression model. Cells  
 390 were supplemented with 20 mM lactate for *S. oneidensis* MR-1 and 20 mM glucose for *E. coli*  
 391 MG1655, no electron acceptor was added. Initial inocula were adjusted to  $OD_{600}$  of 0.01. Data  
 392 show the mean  $\pm$  SD of 3 biological replicates, unpaired two-tailed Student's t-tests were  
 393 performed without adjustments for multiple comparisons, n.s. represents  $p > 0.05$ .  
 394



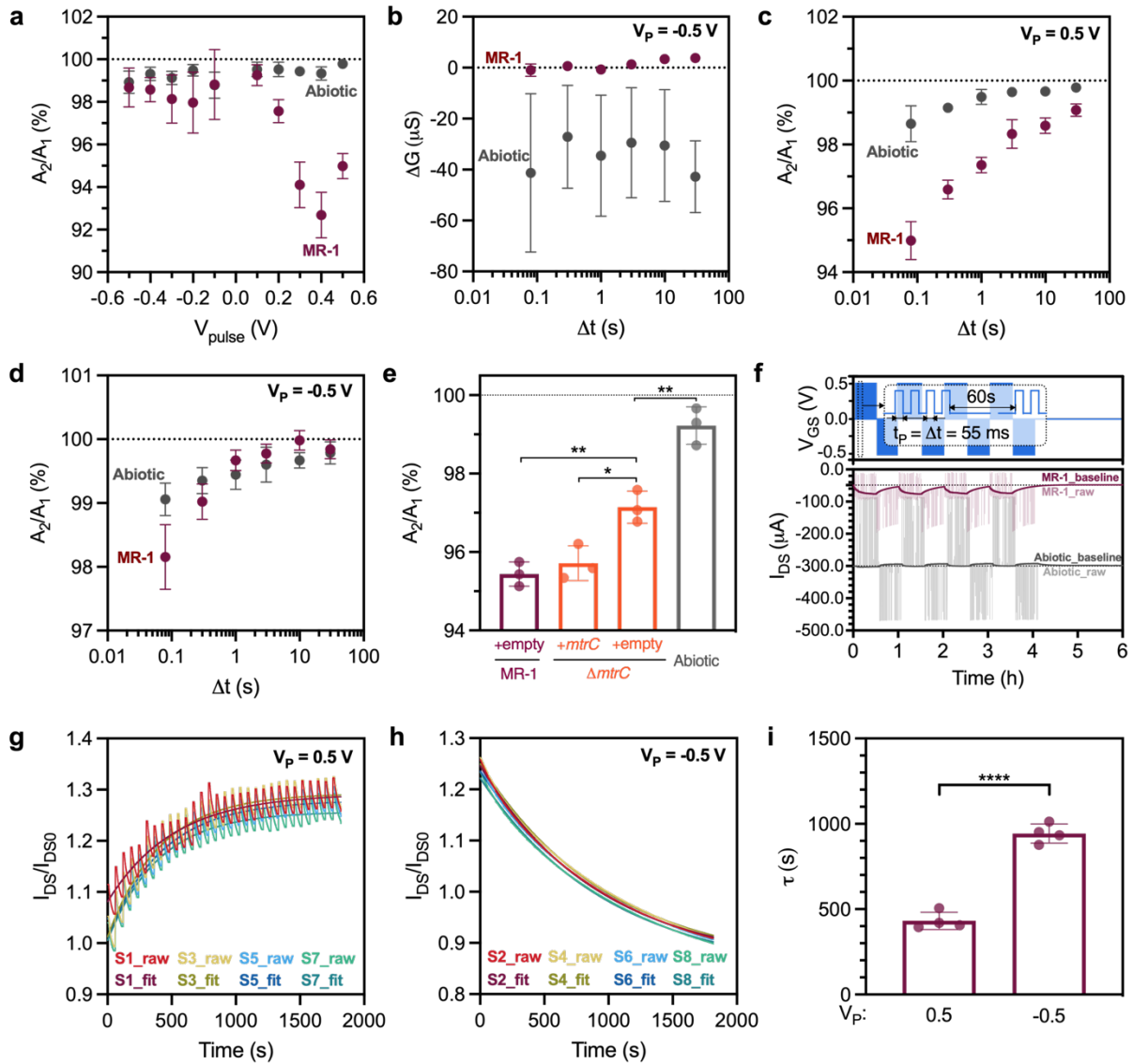
404 cellular extracellular electron transfer (EET) de-doping process of OECT and the 2-electrode  
 405 device. (g) The channel current  $I_{DS}/I_{DS0}$  curves of the 2-electrode devices and OECTs under  
 406 constant gate bias conditions. *S. oneidensis* MR-1 was used for inoculum with an inoculation  
 407 OD<sub>600</sub> of 0.01. Data in panel (g) show the mean  $\pm$  SD of 3 biological replicates. Figure (f)  
 408 created with BioRender.com.

409



410

411 **Figure S4.** OECT responses to  $\Delta mtrC$  strains carrying NAND and NOR Boolean gate plasmids.  
 412 Cartoon illustrations of the plasmid architecture of the (a) NAND and (b) NOR Boolean gates  
 413 expressing  $mtrC$ . The  $\Delta mtrC$  mutants carrying the corresponding Boolean gate plasmids were  
 414 brought to steady-state MtrC expression with combinations of 500  $\mu M$  IPTG, 200 nM OC6, and  
 415 10 nM aTc inducers. Transfer curves of the induced (c) NAND and (d) NOR gates samples. The  
 416 channel current  $I_{DS}/I_{DS0}$  curves for (e) NAND and (f) NOR gates samples with different inducer  
 417 combinations. Data in panels (e) and (f) show the mean  $\pm$  SD of 3 biological replicates. Figure (a)  
 418 and (b) created with BioRender.com.



419

420 **Figure S5.** Modulation of the OECT synaptic behavior with varying pulse conditions and strains.

421 (a)  $A_2/A_1$  index plotted with varying pulse voltage  $V_P$ , while pulse duration  $t_P$  and pulse interval

422  $\Delta t$  were fixed at 80 ms. (b) OECT channel conductance changes  $\Delta G$  with varying pulse interval

423  $\Delta t$ , fixed  $t_P = 80$  ms and  $V_P = -0.5$  V.  $A_2/A_1$  index for OECTs with varying pulse interval  $\Delta t$ , fixed

424  $t_P = 80$  ms and  $V_P$  of (c) 0.5 V or (d) -0.5 V. (e)  $A_2/A_1$  index of  $\Delta mtrC$  strain carrying *mtrC* Buffer

425 gate (+*mtrC*) or empty vector plasmid (+empty) under steady-state protein expression.  $A_2/A_1$

426 index  $p$  values for pairs indicated from top to bottom  $p = 0.0046$ ,  $p = 0.0045$ , and  $p = 0.0149$ . (f)

427 Channel current  $I_{DS}$  responding to the continuous voltage pulses with  $V_P$  of 0.5 V or -0.5 V. Faded

428 lines represent the raw  $I_{DS}$ , while the bolded lines represent  $I_{DS}$  baselines after filtering out the

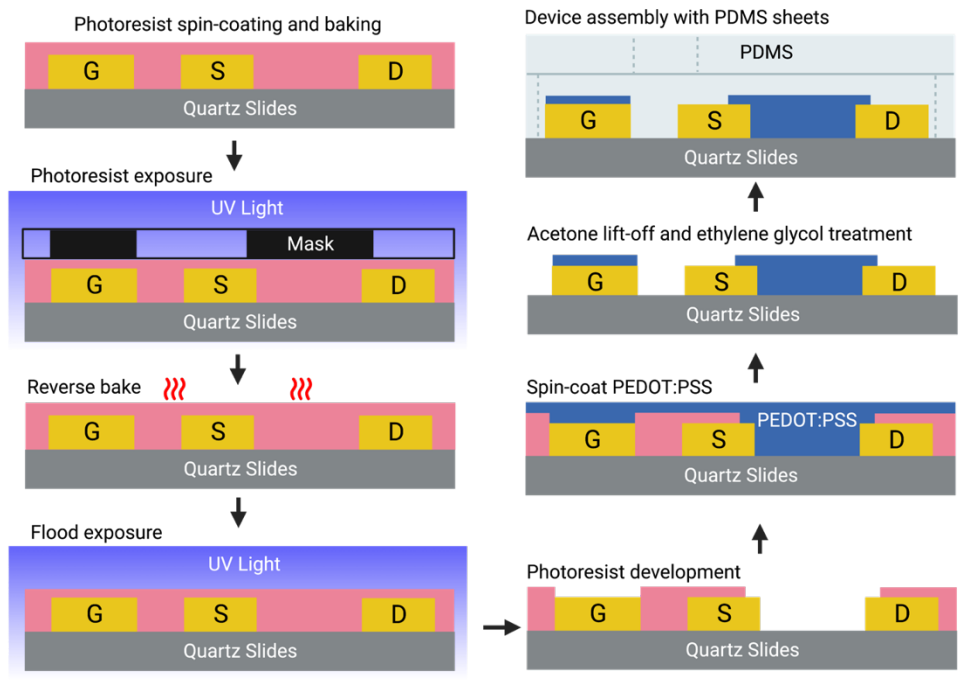
429 pulses. (g, h) One-phase exponential fitting of the  $I_{DS}$  baselines for each continuous 4-pulse

430 session, with  $V_P$  equal to (g) 0.5 V or (h) -0.5 V. (i) The corresponding time constants of the fitting

431 results. Time constant  $p$  values for the indicated pair  $p = 1.0 \times 10^{-5}$ . In panel (a) to (e), data show

432 the mean  $\pm$  SD of 3 biological replicates. In panel (e) and (i), unpaired two-tailed Student's t-tests

433 were performed without adjustments for multiple comparisons, n.s. represents  $p > 0.05$ .



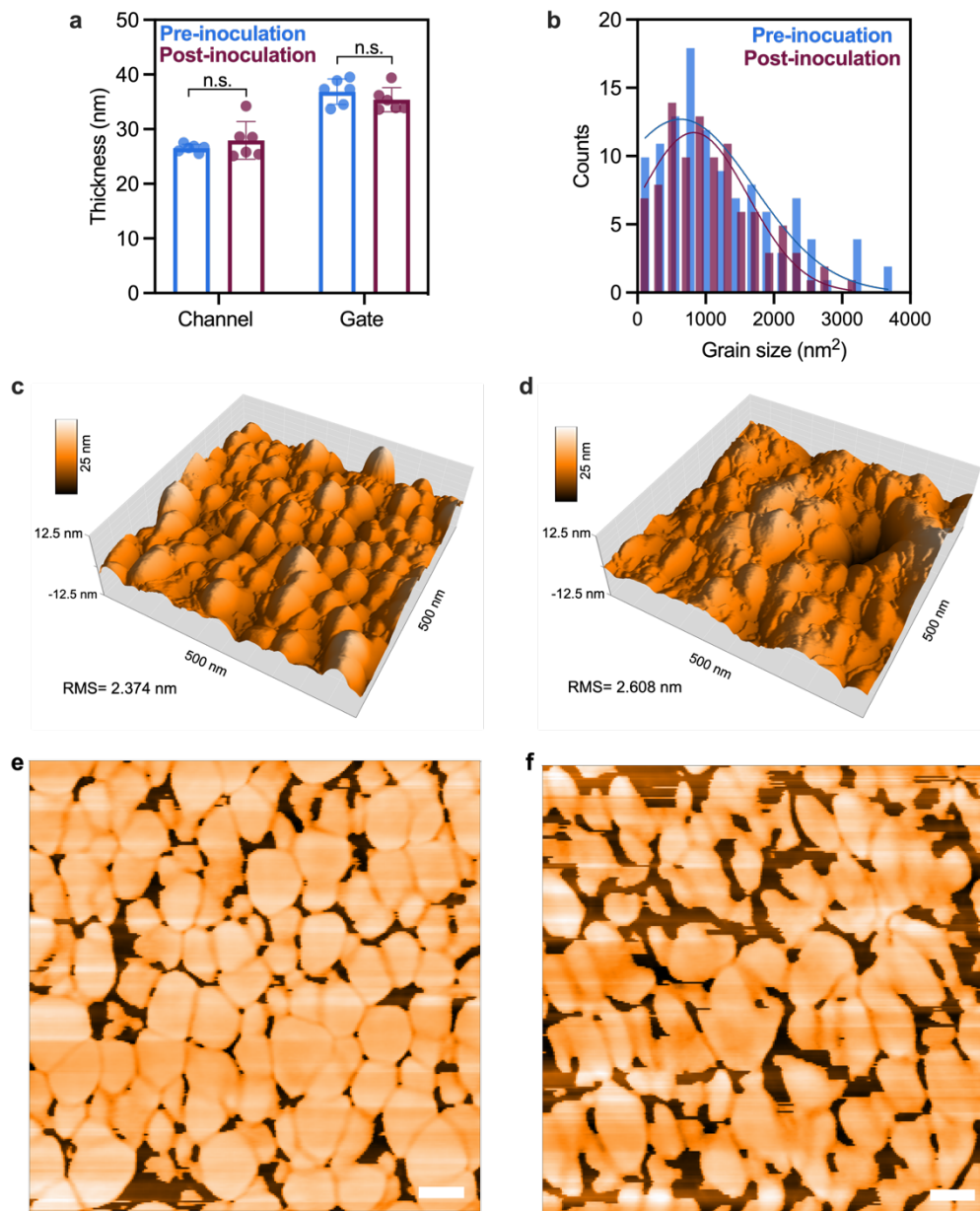
434

435

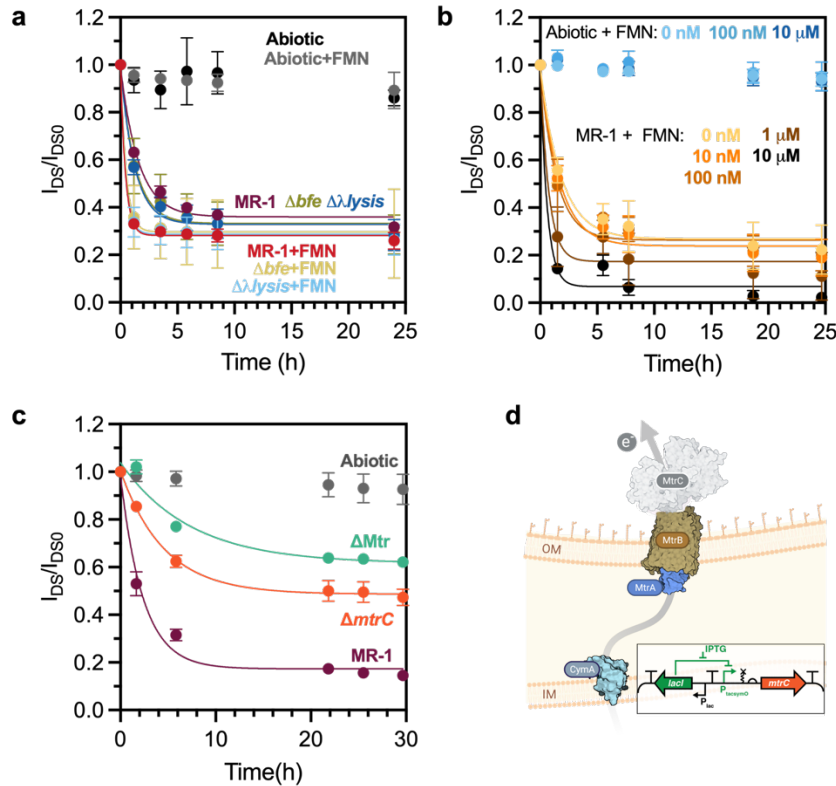
436

**Figure S6.** Cartoon illustration of the major OECT channel fabrication and assembly steps. Created with BioRender.com.





437  
 438 **Figure S7.** Morphological characterization of PEDOT:PSS channel and gate-tip coating.  
 439 (a) Thickness of PEDOT:PSS films derived from AFM scans. OECTs were inoculated with *S.*  
 440 *oneidensis* and operated with constant bias voltages at the gate  $V_{GS} = 0.2$  V and drain  $V_{DS} = -$   
 441  $0.05$  V for 48 hours. (b) Histogram and Gaussian fit (lines) of PEDOT grain size in the channel  
 442 region based on (e) and (f). Representative surface topologies of the PEDOT:PSS channel (c)  
 443 prior to and (d) after the *S. oneidensis* incubation. Representative phase images of the  
 444 PEDOT:PSS channel (e) prior to and (f) after the incubation, scale bars represent 50 nm. AFM  
 445 measurements were performed on 6 independent samples. Panel (c) to (f) presents a zoomed-in  
 446 morphology graph extracted from 2 representative samples. In panel (a), unpaired two-tailed  
 447 Student's t-tests were performed without adjustments for multiple comparisons, n.s. represents  
 448  $p > 0.05$ .  
 449



450

451 **Figure S8.** OECT response to different extracellular electron transfer (EET) mechanisms.

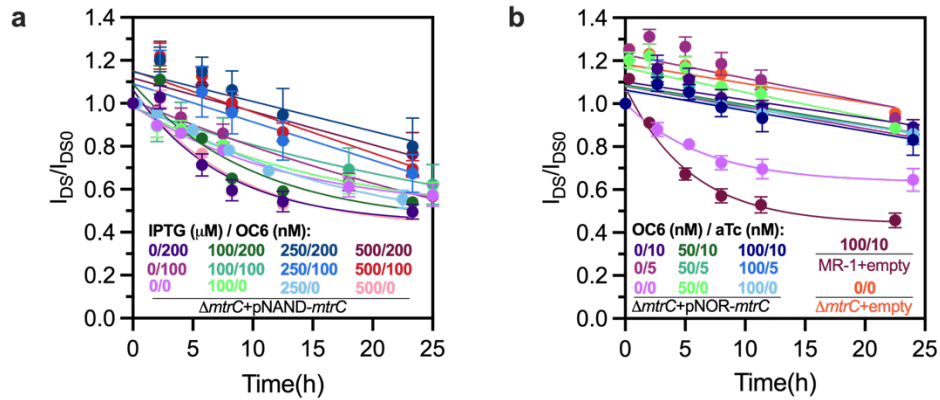
452 (a) The  $I_{DS}/I_{DS0}$  curves of knockout strains with and without the addition of exogenous flavin  
 453 mononucleotide (FMN) ( $1\mu\text{M}$ ), and (b) *S. oneidensis* MR-1 cells with varying exogenous FMN  
 454 concentrations. Initial inocula were adjusted to  $OD_{600}$  of 0.05. (c) The  $I_{DS}/I_{DS0}$  curves of  $\Delta mtrC$ ,  
 455  $\Delta Mtr$ , and MR-1 strains with initial inoculation  $OD_{600}$  at 0.1. (d) Cartoon illustration of the  $\Delta mtrC$   
 456 strain and (d, insert) diagram of the *mtrC* Buffer gate controlled by the IPTG inducer. Faded  
 457 shapes indicate removed proteins with genomic deletion and inhibition of electron transfer through  
 458 the inner (IM) and outer (OM) membranes. Data show the mean  $\pm$  SD of 3 biological replicates.  
 459 Figure (d) created with BioRender.com.

460

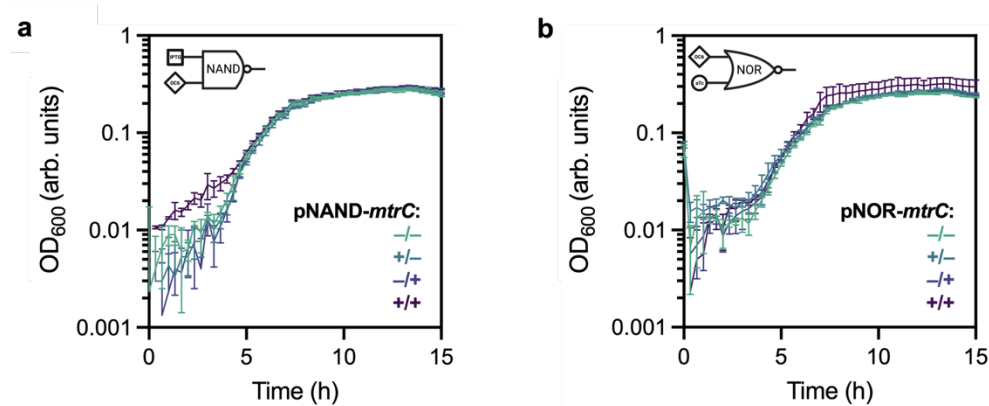
461

462

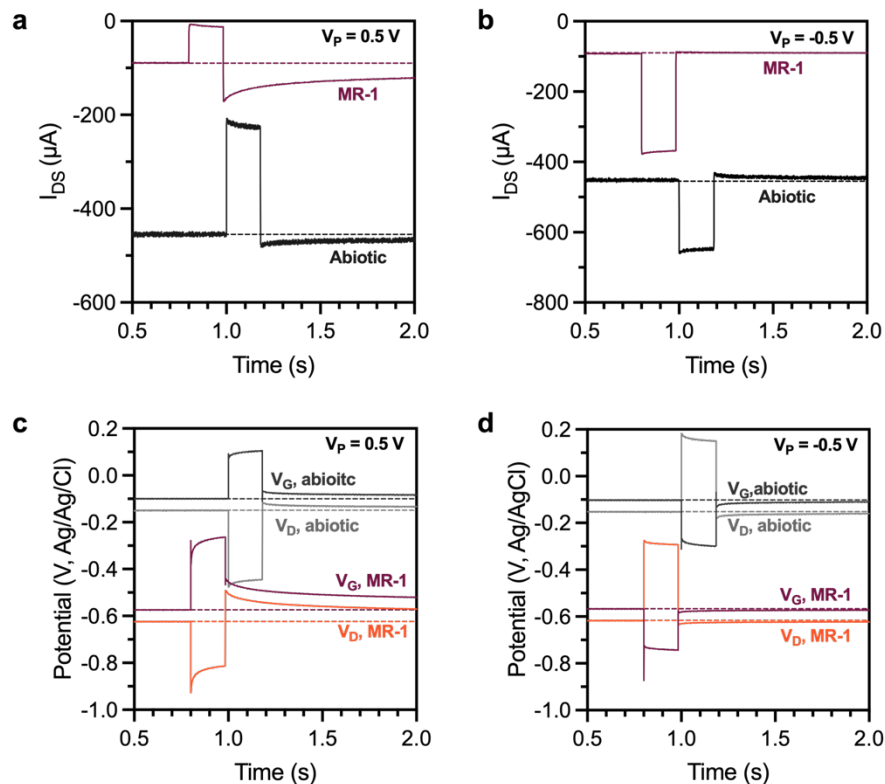
463



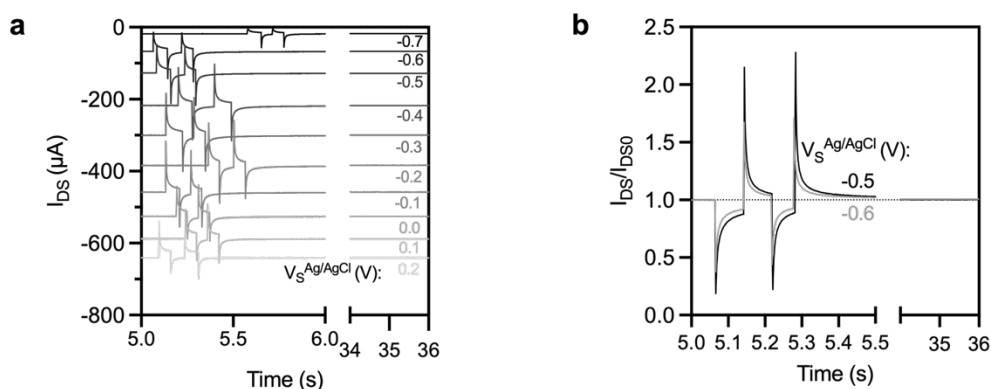
464  
 465 **Figure S9.** Channel current  $I_{DS}/I_{DS0}$  curves of strains carrying the Boolean logic gates plasmids.  
 466 (a)  $\Delta mtrC$  strain carrying NAND Boolean  $mtrC$  plasmids. (b)  $\Delta mtrC$  strain carrying NOR Boolean  
 467  $mtrC$  plasmids. MR-1 strain and  $\Delta mtrC$  strain carrying empty vectors were used as positive and  
 468 negative controls, respectively. Inducible mutants were brought to steady-state expression under  
 469 various inducer combinations and concentrations before inoculation. Data show the mean  $\pm$  SD  
 470 of 3 biological replicates.  
 471



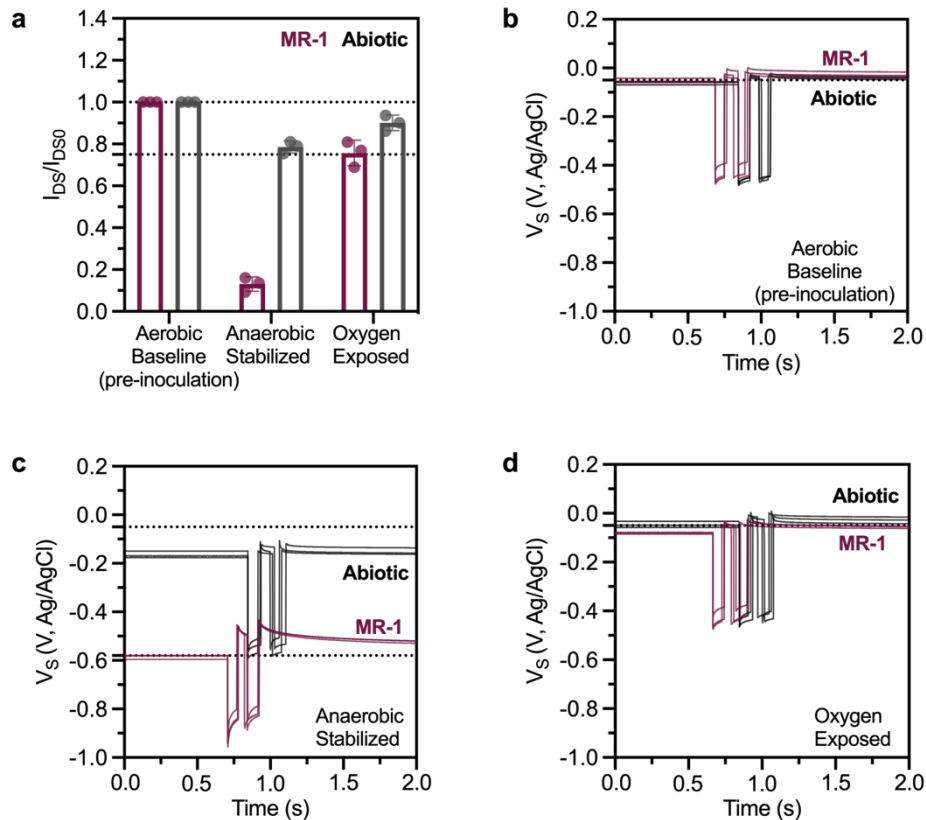
472  
 473 **Figure S10.** Growth curves of mutant strains carrying the Boolean logic gates plasmids.  
 474 (a) NAND or (b) NOR Boolean  $mtrC$  plasmids under different inducer (IPTG, OC6, and aTc)  
 475 combinations. Data show the mean  $\pm$  SD of 3 biological replicates. Created with BioRender.com  
 476



477  
 478 **Figure S11.** Measured channel currents  $I_{DS}$  and electrode potentials responding to gate pulses.  
 479 Single gate pulses with pulse duration  $t_p = 1.5$  s, pulse voltage  $V_P$  equal to (a, c) 0.5 V and (b, d)  
 480 -0.5 V were applied between gate and source electrodes while constant drain voltage  $V_{DS} = -0.05$   
 481 V was applied. Gate potential  $V_G$  and drain potential  $V_D$  were measured against Ag/AgCl pseudo-  
 482 reference electrodes.  
 483



484  
 485 **Figure S12.** Paired-pulse responses of abiotic OECTs at varying electrochemical doping states.  
 486 The source electrode potential ( $V_S$ ) was constantly biased at the specified voltages against the  
 487 Ag/AgCl pseudo-reference electrode. (a) Channel current  $I_{DS}$  of OECT with  $V_S$  biased from 0.2 V  
 488 to -0.7 V in increment of 0.1 V. (b) Normalized  $I_{DS}$  for  $V_S$  biased at -0.5 V and -0.6 V.  
 489



490  
 491 **Figure S13.** Electrochemical response of the hybrid OECTs under varying oxygen conditions.  
 492 (a) Channel current  $I_{DS}$  were normalized to the pre-inoculation aerobic baseline values, with gate  
 493 voltage  $V_{GS} = 0$  V and drain voltage  $V_{DS} = -0.05$  V. Paired pulse responses of pulse voltage  $V_P =$   
 494  $0.5$  V and drain voltage  $V_{DS} = -0.05$  V were shown with the measured source electrode potentials  
 495 against Ag/AgCl pseudo-reference electrode during (b) aerobic pre-inoculation condition, (c)  
 496 anaerobic stabilization post-inoculation, and (d) subsequent re-oxygenation to ambient conditions.  
 497 Data in panel (a) show the mean  $\pm$  SD of 3 biological replicates.

## 498 References

- 499
- 500 1 Yoo, B., Dodabalapur, A., Lee, D. C., Hanrath, T. & Korgel, B. A. Germanium nanowire  
 501 transistors with ethylene glycol treated poly(3,4-ethylenedioxythiophene): poly(styrene  
 502 sulfonate) contacts. *Applied Physics Letters* **90** (2007). <https://doi.org/Artn> 072106  
 503 10.1063/1.2535710
  - 504 2 Muller, J., Shukla, S., Jost, K. A. & Spormann, A. M. The mxd operon in *Shewanella*  
 505 *oneidensis* MR-1 is induced in response to starvation and regulated by ArcS/ArcA and  
 506 BarA/UvrY. *Bmc Microbiology* **13** (2013). <https://doi.org/Artn> 119  
 507 10.1186/1471-2180-13-119
  - 508 3 Coursolle, D. & Gralnick, J. A. Modularity of the Mtr respiratory pathway of *Shewanella*  
 509 *oneidensis* strain MR-1. *Molecular Microbiology* **77**, 995-1008 (2010).  
 510 <https://doi.org/10.1111/j.1365-2958.2010.07266.x>

- 511 4 Coursole, D. & Gralnick, J. A. Reconstruction of extracellular respiratory pathways for  
512 iron(III) reduction in *Shewanella oneidensis* strain MR-1. *Frontiers in Microbiology* **3**  
513 (2012). <https://doi.org/ARTN> 56  
514 10.3389/fmicb.2012.00056
- 515 5 Kotloski, N. J. & Gralnick, J. A. Flavin Electron Shuttles Dominate Extracellular Electron  
516 Transfer by *Shewanella oneidensis*. *Mbio* **4** (2013). <https://doi.org/ARTN> e00553-12  
517 10.1128/mBio.00553-12
- 518 6 Binnenkade, L., Teichmann, L. & Thormann, K. M. Iron Triggers lambda So Prophage  
519 Induction and Release of Extracellular DNA in *Shewanella oneidensis* MR-1 Biofilms.  
520 *Applied and Environmental Microbiology* **80**, 5304-5316 (2014).  
521 <https://doi.org/10.1128/Aem.01480-14>
- 522 7 Dundas, C. M., Walker, D. J. F. & Keitz, B. K. Tuning Extracellular Electron Transfer by  
523 *Shewanella oneidensis* Using Transcriptional Logic Gates. *Acs Synthetic Biology* **9**,  
524 2301-2315 (2020). <https://doi.org/10.1021/acssynbio.9b00517>
- 525 8 Graham, A. J. *et al.* Transcriptional Regulation of Synthetic Polymer Networks. *bioRxiv*,  
526 2021.2010.2017.464678 (2021). <https://doi.org/10.1101/2021.10.17.464678>  
527